

# Multiejector CO<sub>2</sub> cooling system with evaporative gascooler for a supermarket application in tropical regions

Simarpreet Singh<sup>(a)</sup>, Armin Hafner<sup>(b)</sup>, M.P. Maiya<sup>(a)</sup>, Krzysztof Banasiak<sup>(b)</sup>, Petter Neksa<sup>(c)</sup>

<sup>(a)</sup>Indian Institute of Technology Madras, India

<sup>(b)</sup>Norwegian University of Science and Technology, Norway

<sup>(c)</sup>SINTEF Energy Research, Norway

## Abstract

In the present study, the performance of a 33 kW multiejector trans-critical CO<sub>2</sub> cooling system is experimentally evaluated for a supermarket application with/without internal heat exchanger and evaporative cooling. In order to enhance the overall performance of the system for tropical regions, the testing is carried out at high ambient temperature (up to 46°C) with 5cm, 10cm and 15cm cooling pad thickness arrangements. The experimental results clearly projects that the evaporative cooler capacity reaches a maximum of 10cm pad thickness. However, a minor improvement is observed in terms of Coefficient of Performance and Power Input Ratio beyond 10cm pad thickness. Maximum improvement in COP with internal heat exchanger and evaporative cooler is 11% and 40% respectively. On the other hand, a maximum reduction in the system Power Input Ratio with internal heat exchanger and evaporative cooler is 8.5% and 26% respectively. However, a minor enhancement in Coefficient of Performance and Power Input Ratio of 4% and 6% are observed respectively with 15cm cooling pad thickness. Furthermore, a comparative analysis is carried out with the existing and present experimental study to project the compatibility of an evaporative condenser in the ejector based CO<sub>2</sub> cooling system. From the study, it is evident that the evaporative cooling arrangement for the gascooler of the CO<sub>2</sub> system is suggested as a potential solution to the supermarket application at a high ambient temperature context.

**Keywords:** Evaporative cooling, Internal heat exchanger, Power Input Ratio, Supermarket.

## 1. Introduction

In 1919, CO<sub>2</sub> cooling technology was quite commonly used for refrigeration applications for large spaces with dense human population, areas such as theatres, departmental shops, stores, etc. in cold regions of advanced countries [1]. It was further expanded to churches, and then to air conditioning systems in 1925. The technology became so popular that 80% of ships installed non-toxic CO<sub>2</sub> vapor compression cooling systems while 20% opted for an ammonia-based vapor absorption refrigeration system. In 1928, CFCs were introduced with a huge promotion campaign as a replacement for natural working refrigerants with their low-pressure operations and increased system working efficiency [2]. R12 and R11 were first introduced and endorsed in 1931 for fully commercial applications. The main reason for the disappearance of the CO<sub>2</sub> technology is due to the lack of advancement in the technology for natural working refrigerants besides the considerable service needs and maintenance effort for the units. Also, the physical property limitation

challenges like low critical temperature (31.1°C) and high critical pressure (7.1 MPa) of CO<sub>2</sub> cause significant system efficiency losses in conventional cycles and many other problems associated with the design of various components. Therefore, by the 1950s, most of the cooling systems working with CO<sub>2</sub> were replaced with synthetic refrigerants [3].

In the early 1990s, due to the amendment and outline of Montreal protocol and Kyoto protocol, the phase-out of synthetic (man-made) refrigerants was initiated to prevent global warming issues and as a result, CO<sub>2</sub> based natural refrigeration technology went through/faced a revival in the HVAC&R sector. In 1994, Prof. Gustav Lorentzen in NTH, Norway proposed and demonstrated CO<sub>2</sub> cooling technology as the best alternative to synthetic refrigerants for various applications such as automobile air conditioning, domestic hot water heat pumps, and for simultaneous heating and cooling applications [4].

In CO<sub>2</sub> systems, the gascooler is reported to be the most influential module to help achieve the overall required performance of the system. Several attempts were made by using air and water (heat sinks) as heat transfer medium in CO<sub>2</sub> gascooler. Substantial research work focussing on various condenser/gascooler designs was also reported and among them, a few gascooler designs have already been commercialized for heat pumps and refrigeration applications in colder climates for its ambient operating conditions [5]. Moreover, several attempts were carried out to explain the effect of the evaporative cooling principle on the improved overall performance of the refrigeration system for different ambient temperature conditions (high and low ambient temperature conditions). However, a very few studies are reported for the CO<sub>2</sub> refrigeration system with an evaporative condenser. Therefore, it is important to study the influence of adopting the evaporative cooler on the overall performance of the CO<sub>2</sub> gascooler. Also, the influence on its capacity, to promote the applicability of the natural working refrigerant based CO<sub>2</sub> refrigeration system for tropical conditions (high ambient temperature conditions) under transcritical operation.

### **1.1. Literature review**

In the literature, various experimental equipment improvement studies have been reported with different approaches to effective gascooler designs. A study was carried out applying a CO<sub>2</sub>/water coupled micro-channel gascooler for a heat pump water heater application [6]. During the study, a simulation model was developed and validated using the experimental results obtained. It was reported that the impact of refrigerant side thermal resistance decreased near pseudo-critical point during the high pressure operation (supercritical operation). Later, a tube-in-tube CO<sub>2</sub> gascooler design was developed and tested for the supercritical operation adopting a water heat pump application [7]. It was reported that the effect of the inlet pressure of the gascooler on the temperature drop was not as apparent as the effect of the inlet pressure on the heat transfer rate. However, a significant improvement in the overall heat transfer coefficient was reported for the same.

A fin-tube design gascooler for transcritical CO<sub>2</sub> cooling systems was developed for warm weather conditions, to comparatively analyze the various operating parameters such as approach temperature, refrigerant side pressure drop, air velocity, etc. [8]. Further guidelines were proposed after this exchanger performance study, to design a fin-tube CO<sub>2</sub> gascooler for high ambient temperature operation. A later study proposed two different alternatives of CO<sub>2</sub> fin-tube design with a gascooler/condenser. The same was tested in a CO<sub>2</sub> booster refrigeration system configuration [9]. Moreover, a simulation model was also developed to analyse the varied ambient conditions and validated with the obtained experimental results. The study reported a detailed prediction of the working fluid's necessary outlet temperature profiles as well as the overall effect of different pipe circuitry arrangements for achieving improved heat transfer rate. Later, a pilot study was carried out using a fin-tube gascooler/condenser with CO<sub>2</sub> booster refrigeration system configuration [10]. It was observed that, when a large size gascooler was utilized for a constant ambient temperature operation, the optimum available pressure level in the gascooler was reduced, however, it achieves a smaller approach temperature during the operation.

In order to observe the enhanced effects of counter cross-flow pattern in a tube-in-tube design gascooler and its overall effect on the system performance, a new model was proposed and also, validated with the support of an experimental study for the CO<sub>2</sub> heat pump application [11]. The drastic rise of the specific heat property of CO<sub>2</sub> with reduced temperature was reported which was responsible for the increased local heat transfer coefficient. Moreover, it was observed that the gascooler tube side performance peaked near the pseudo-critical region. A twisting turbulence enhancement in the tube-in-tube gascooler of the CO<sub>2</sub> unit was reported for the heat pump water heater application [12]. During the study, two different coil twisting designs were analyzed and compared. It was observed that the pressure drop, and the overall heat transfer rates increased significantly due to an increase in the number of twists in the tubes.

It could be determined that there have been many attempts reported to design, analyzed, proposed and test the various types of heat exchangers to improve the performance of the CO<sub>2</sub> refrigeration system. However, very limited research work is reported with evaporative cooling principle for the CO<sub>2</sub> technology, which is infact a promising option for the tropical regions. Five decades ago, the evaporative cooling principle was introduced in the refrigeration cooling system. Since then, several types of direct and indirect evaporative cooler designs were proposed and experimentally tested for various ambient temperature conditions. A few important studies related to the present work concerning the evaporative cooling principle is reported to project the current research scenario. The evaporative cooling principle was introduced for the CO<sub>2</sub> refrigerant cooling system to improve the heat transfer characteristics and the overall performance of the CO<sub>2</sub> gascooler operating in sub-critical conditions [13]. It was reported that, using cooled moist air as the heat transferring medium in precooling, results in a promising improvement in its overall heat transfer coefficient and consequent system performance for various applications. A simulation-based study was reported to analyze the effect of both direct and indirect evaporative coolers for variable

domestic cooling loads for the Iraq dwelling [14]. The concept of was introduced as a control strategy to analyze the variable cooling load handling by the system. The performance of the system with indirect evaporative cooling was reported higher than the other.

The energy-saving potential of the indirect evaporative cooling was introduced in Kuwait with the support of varying weather conditions [15]. Through the proposed module of the system, the energy saving for the cooling system was reported higher than the coastal area. An experimental study was carried out with the direct evaporative cooler arrangement for the peak summer weather in a Brazilian city [16]. Moreover, a mathematic model was proposed as an outcome which could provide the effectiveness of direct evaporative cooler with high accuracy for various operating conditions. Furthermore, a few studies were carried out employing the evaporative condenser in the simple vapor compression refrigeration configuration. A simulation model of spray air-cooled condenser was proposed, which was further coupled with the refrigeration system to observe its influence as compared to the dry cooled condenser for low ambient air temperature conditions ( $\sim 25^{\circ}\text{C}$ ) [17]. It was reported that the COP of the refrigeration system working with R404A was increased by 55%, thus concluded a potential solution to improve the efficiency of the refrigeration system.

An experimental study was reported using the direct/indirect design of the evaporative cooling pad for various climate conditions in Iran [18]. With the two primary motives of comfort air conditioning and system power savings. The study was carried out based on providing the optimum water supply ratio to the direct evaporative cooling system. More than 60% of power saving with comparison to the simple vapor compression refrigeration system was reported with 55% increment in water consumption. Another theoretical model for direct evaporative cooler was proposed with a simplified correlation for the cooling efficiency based on the energy balance analysis of the air [19]. The influence of the frontier air velocity and the cooling pad thickness on the cooler performance was considered. An optimum air velocity of 2.5 m/s was reported to decide the frontal area of the cooling pad. Later, a ground assisted evaporative cooling pad for Tehran was analyzed to provide the pre-cooling effect to the air used in the direct evaporative cooler [20]. With the support of a simulation-based study with the hybrid approach used for the direct evaporative coolers, more than 100% efficiency improvement was reported as compared to the mechanical simple vapor compression refrigeration system.

A simplified model to discuss the heat and mass transfer between air and water in a direct evaporative cooler was proposed [21]. The optimum solution for the mathematical model design was reported concerning the frontal air velocity, cooling pad thickness, and air-dry bulb temperature. The thermal analysis of a novel integrated system with a ground heat exchanger for the precooling of the air to the direct evaporative cooler was carried out [22]. It was reported that the proposed design could significantly reduce the air inlet temperature below the wet-bulb temperature and is highly efficient for air conditioning applications. Another study was reported

employing evaporative condenser with the vapor compression refrigeration system [23]. The experimental study was carried out with the dual independent evaporative cooler design for a single stage R134a vapor compression refrigeration system. An increment of 13.1% in system COP was reported with the evaporative condenser configuration.

In 2016, an experimental study was carried out for the CO<sub>2</sub> ground heat pump system with both air and water cooler condenser/gascooler for high ambient temperature conditions [24]. The experimental results were also compared with the R134a refrigeration system. With the proposed design the cost of the system was reduced by 14.7% as reported. In the same year, another experimental study was reported with evaporative cooling for a split air conditioning system coupled with its outdoor unit and using R407C refrigerant [25]. It was reported that the reduction in compression power and increment in cooling capacity by 11.4% and 1.8% respectively. A new design concept of an evaporative cooler with internal baffles was proposed with the support of numerical and experimental study [26]. Five variations in the baffles designs w.r.t. the airflow path was studied and a maximum 43% improvement in efficiency was reported.

An experimental study was carried out by coupling the simple vapor compression (R22) split air condition system's outdoor unit with the evaporative cooler [27]. It was reported that the reduction in the compressor power and enhancement in the system COP were 6.1% and 21.4% respectively. Moreover, the study concluding evaporative cooling as a reliable option to improve the overall system performance. Later, the evaporative cooling was adopted for the automotive air conditioning application, and performance was evaluated based on a model developed with the support of a genetic algorithm multi-objective technique [28]. Four passes louvered fin-flat tube condenser was modelled and increment in the overall heat transfer effect and decrement in pressure drop was 4 % and 8 % respectively was reported. A simplified model for the reduction in the water consumption for the evaporative cooling pad was also proposed and experimentally validated for the direct evaporative cooler [29]. Saline water with different concentrations was used as the feed water and reported the reduction of 1.5 litres/hour of water consumption, however, the supply air temperature was increased by 8.6%. A study was reported for the performance evaluation of a direct evaporative cooling system for Indian operating conditions with the support of experimental results [30]. Aspen and honeycomb cooling pads were used to compare the system performance. The honeycomb cooling pad was reported as the most suitable option for the dry and warm climatic conditions in India. In the same year, a new concept of pillow-plate heat exchanger for the process industries was proposed and evaluated with the support of experimental results, and the design was reported as a promising alternative to the conventional equipment in the various process industries [31].

Another concept of the indirect evaporative cooler with the combination of internal baffles and evaporative condenser was proposed [32]. The experimental study was conducted and a 54% improvement in the cooling capacity was reported. In the same year, the performance of a finned

tube condenser/gascooler was evaluated with the support of an experimental study for the CO<sub>2</sub> refrigeration system with booster configuration [33]. With the support of the various test results, field data analysis, and condenser/gascooler design, it was reported that the CO<sub>2</sub> is the potential substituent for the R404 refrigerant in supermarket applications but below 31°C ambient temperature conditions or in sub-critical conditions. A hybrid combination of the evaporative cooler in the desiccant cooling system was proposed and the study was also supported with the experimental results [34]. The system with this hybrid combination was reported as 60% more efficient than the simple vapor compression cooling system. A concept of regenerative indirect cooler with high/low control was proposed and evaluated with the on/off control system [35]. Also, a control strategy was developed and evaluated to control the influence of ambient air conditions. Maximum 13.1% energy saving was reported by the proposed on/off strategy.

An experimental study was carried out at a subway station in Beijing, China in order to evaluate the enhancement in the air conditioning system performance using evaporative condenser [36]. It was reported that the evaporative cooler arrangement for the cooling system appeared as a feasible solution in terms of energy efficiency, operational cost and carbon emission. Later, thermal performance of a vertical tube evaporative condenser as a replacement of the air-cooled condenser was reported with the support of a computational and experimental observations. Overall improvement in the COP of the system was reported as 30% [37]. An experimental study was carried out for the heat and mass characteristics of an evaporative condenser with a horizontal elliptical tube bundle [38]. An empirical correlation was finally proposed using the experimental data in order to evaluate the overall performance and the heat transfer characteristics of the condenser tube. Recently, in 2020, an experimental study was carried out to improve the overall performance of a small-scale domestic water-cooling system using water cooled condenser in tropical region [39]. It was reported that the maximum reduction in the energy consumption and total equivalent warming impact were 27% and 26.8% respectively. With the support of an artificial neural network model and design of experimental tool, performance evaluation of an evaporative condenser was carried out for various operating conditions [40]. In the study, a unique methodology was proposed as a useful tool in order to develop a simulated complex system in a much easier way.

## **1.2. Study objectives**

Studies reported for different cooling pad design used for the evaporative condensers are tabulated in Table 1. The various alternative material designs of cooling pads used so far are also tabulated along with the quantified maximum improvement observed for various ambient temperature conditions. After an extensive literature survey, it has been observed that no study was reported with the CO<sub>2</sub> evaporative gascooler refrigeration system with honeycomb cooling pad material for tropical regions (high ambient temperature conditions). Thus, it is interesting and important to study the performance improvement of the CO<sub>2</sub> refrigeration system with the support of

evaporative gascooler arrangement with honeycomb cooling pad design to promote the applicability of the natural working refrigerant CO<sub>2</sub> technology for the tropical regions like India.

## 2. Ambient temperature conditions during experiments

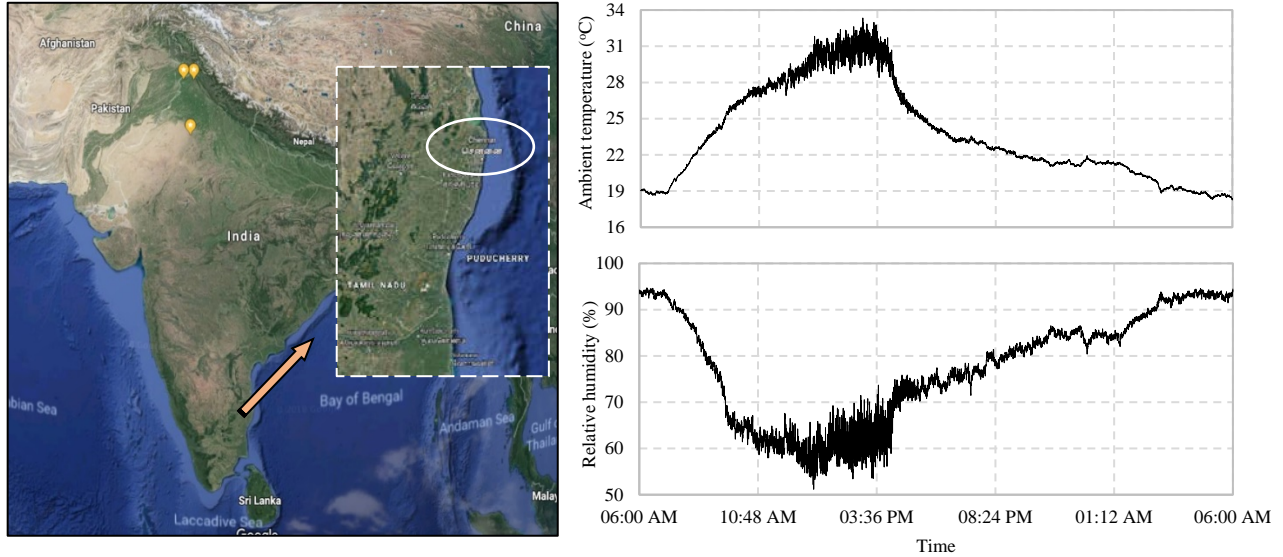


**Figure 1 (a). The location of CO<sub>2</sub> supermarket test-rig**  
**Figure 1 (b). The ambient conditions during the test.**

Fig. 1(a) shows the location of CO<sub>2</sub> supermarket test-rig and Fig. 1 (b) shows the ambient conditions during the test. It is installed in Chennai, India where the average ambient temperature conditions are high as shown. The location is selected to evaluate the performance of the system for the high ambient temperature. Chennai has quite hot and humid weather conditions which allows extreme weather conditions for the test-rig. The temperature and humidity are observed for a period of 24 hours. The peak weather time described is between 10:00 AM to 4:00 PM which is taken into consideration while conducting the experimental work.

**Table 1. Studies reported for different cooling pad design used for the evaporative condensers.**

Reference(s)	Design	Study focus	Pad design	Air temperature	Remarks
[15]	Indirect cooler	Performance evaluation for indirect evaporative cooling	Water absorbent material	35°C	High energy saving was observed (6320 kWh)
[18]	Direct/indirect	Effect of optimum water consumption ratio on the overall performance	Water absorbent material	23°C	60% power savings was reported with the increment of 55% water consumption
[23]	Direct cooler	Proposed an air conditioning system using a dual independent evaporative condenser	Honeycomb	35 °C	COP increased by 13.1% with the air velocity increasing from 2.05 to 3.97 m/s
[25]	Direct cooler	The condensing unit was modified by coupling evaporative cooling pads with a variable pad thickness	Honeycomb	30 °C	COP was enhanced by 10.6% as compared to the conventional system
[26]	Indirect cooler	Proposed a new configuration of indirect evaporative cooler	I-Shape channels	35 °C	System performance was improved by 20.5%
[31]	Direct cooler	Condensation-evaporation process in a pillow plate was studied experimentally	Pillow plate	31.1 °C	Evaporation process in natural circulation model was stable throughout the experiments
[32]	Indirect cooler	Influences of the pre-cooling unit and the external thin-film cotton layer on the performance	Honeycomb	35 °C	The performance was observed to be between 35.4% and 54.2%
[41]	Direct cooler	Comparative performance of cross-flow and counter-flow M-cycle heat exchangers	Rectangular and triangular channels	25 °C	Demonstrated better cooling effectiveness (15% for dew-point and 23% for wet-bulb)



### 3. CO<sub>2</sub> supermarket test-rig facility with an evaporative cooler

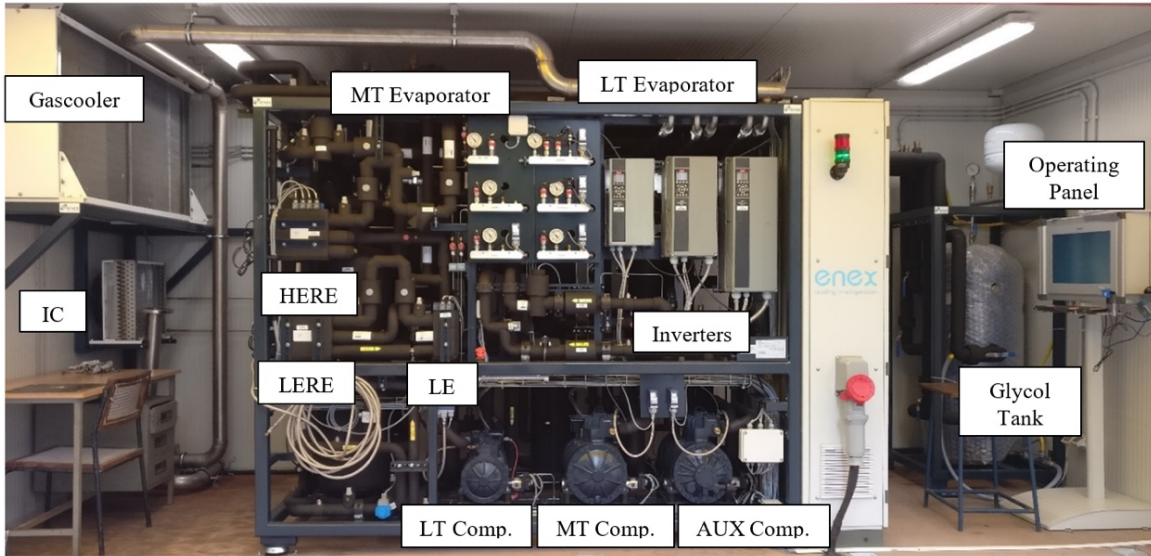


Figure 2. Picture of the CO<sub>2</sub> cooling system test-rig.

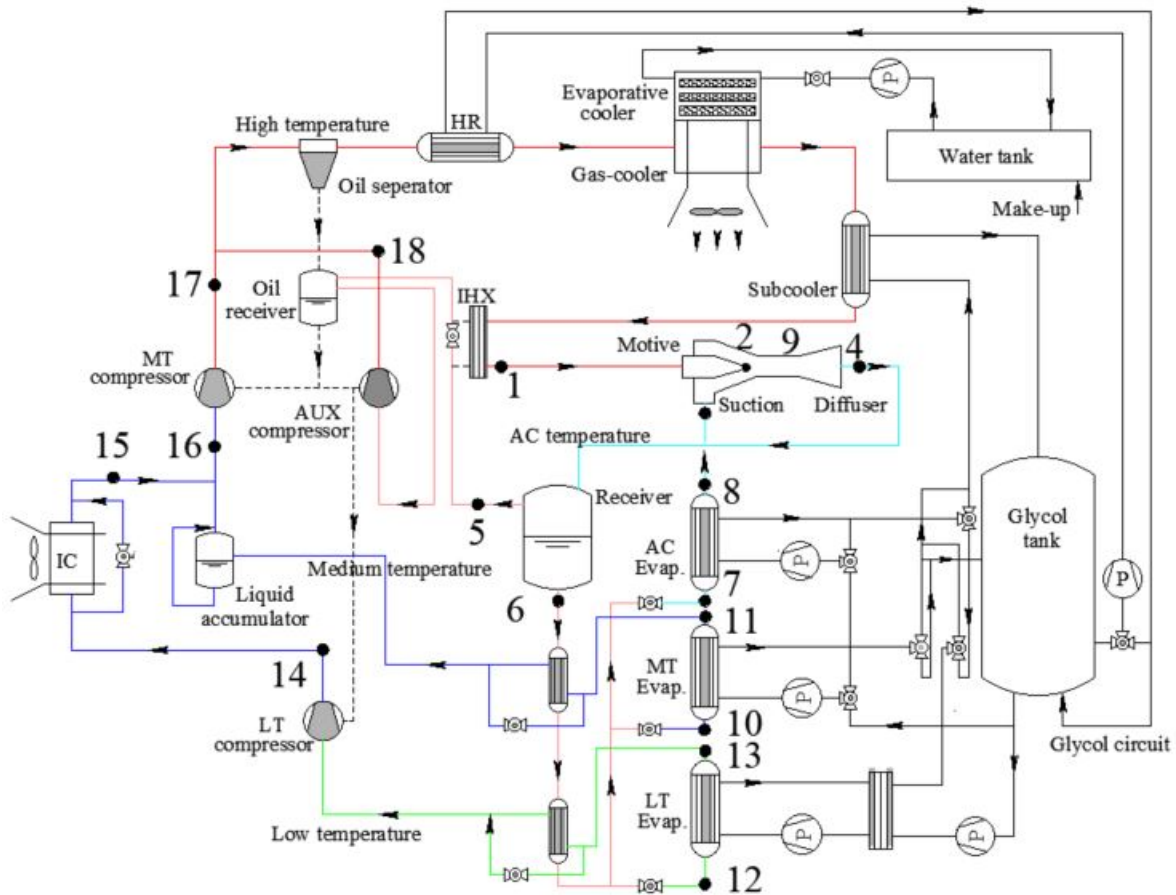
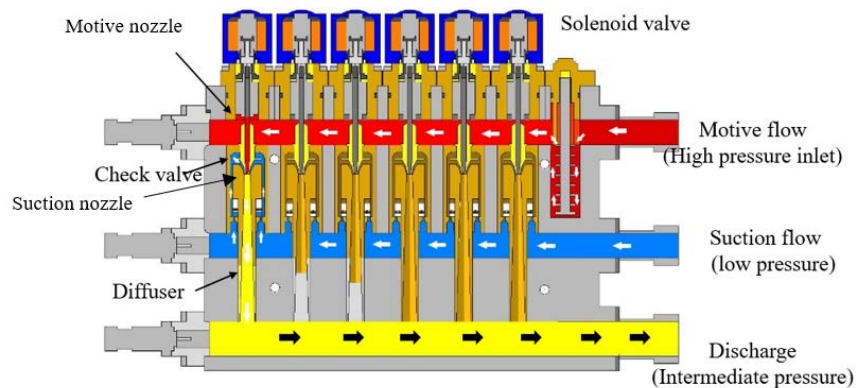


Figure 3. Schematic of the CO<sub>2</sub> cooling system test-rig.

Fig. 2 shows the picture of the CO<sub>2</sub> cooling system test-rig and Fig. 3 shows the schematic of the CO<sub>2</sub> cooling system test-rig. The various pressure levels in the system are highlighted in different colors. The compressor oil collection point in the CO<sub>2</sub> loop is also presented. The rig is fully instrumented and designed with a cooling capacity of 33 kW for supermarket cooling application to maintain three different evaporation temperature levels: -28°C for freezing (LT), -6°C for refrigeration (MT) and +6°C for air conditioning (AC). The test facility is equipped with a heat reclaim (water-glycol solution), which is used to generate heat load towards the three evaporators from the water-cooled gascooler in a closed loop with a glycol reservoir tank.

Two water-glycol loop circuits are arranged with different glycol concentrations according to the cooling application (MT and LT). A load of medium temperature (MT) and low temperature (LT) evaporators on the secondary loop are operated by manually controlled EEVs. The temperature of LT and MT is controlled by compressor suction. The temperature level of the AC evaporator is controlled by the receiver pressure. Three compressors are arranged, LT and MT compressors, and an additional AUX (AC) compressor are installed to handle high amounts of flash gas from the receiver which also enables so-called parallel compression. Three separate inverters are installed to control the compressor motor frequency to achieve the individual set-points. Two multiejectors are installed: one with a low ejection ratio ejector (LERE) and another with a high ejection ratio ejector (HERE). Each ejector has six slots or cartages to control the load variation in the system.



**Figure 4. The internal structure of a two-phase multi-ejector.**

Fig. 4 shows the internal structure of a two-phase multi-ejector that is used in the CO<sub>2</sub> cooling supermarket test-rig. The significant function of the various internal parts of the multi-phase ejector is; the solenoid framed on the top regulates the opening and closing of the solenoid valve of the cartage according to the capacity of the test-rig requested by the opening degree of the high-pressure expansion valve of the system. As the magnet energizes in the solenoid controller, the respective cartage needle lifts results in the valve opening, which further allows the high-pressure refrigerant to enter through the motive nozzle of the ejector. Due to which, low pressure is generated at the suction nozzle, which results in the lifting of the check valve of the suction nozzle, which allows the fluid to enter the mixing chamber. Both motive and suction fluids blends in the

mixing section of the ejector and high kinetic energy are formed in the motive stream before mixing. The mixture enters the diffuser section and the high kinetic energy is converted into pressure energy and the pressure increases to intermediate or discharge pressure which is more than the suction pressure. The difference between these two is known as the ejector pressure lift.

A liquid suction accumulator is also installed to enable a secure separation of liquid and vapor upstream of the compressors to allow a liquid overfeed operation or flooding operation of the evaporators throughout the year. Temperature sensors, pressure sensors, and energy meters are installed at various pressure levels of the test-rig to measure and evaluate the performance of the system and examine the various parameter variations. The system facilitates both manual and automatic optimization of the gascooler pressure level concerning the gascooler outlet temperature. The test-rig facility also has a manually operated controller for the RPM of the two gascooler fans to maintain various airflow rates to manipulate or adjust the refrigerant exit temperature in the gascooler. Details of the various sensors installed in the CO<sub>2</sub> test-rig are tabulated in Table 2.

**Table 2. Various sensors installed in the CO<sub>2</sub> test-rig.**

S. no.	Sensor	Brand	Model	Type	Range	Accuracy (% of measure value)
1.	Temperature	Danfoss	AKS 21M	B	-50 to 200°C	0.4
2.	Pressure	Danfoss	AKS 2050	----	up to 150 bar	0.5
3.	Energy meter	ISOIL	PT 500	IFX-M	3.0 m <sup>3</sup> h <sup>-1</sup>	0.5
4.	Power meter	Danfoss	VFD	----	35-60 Hz	0.8

### 3.1. Supermarket operation of the test-rig

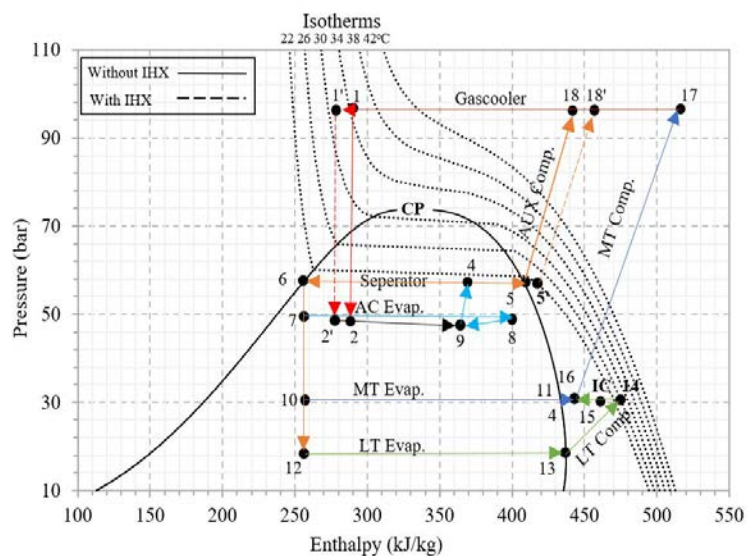


**Figure 5. Ph plot of the supermarket operation of the CO<sub>2</sub> test-rig**

Fig. 5 shows the  $Ph$  plot of the supermarket operation of the CO<sub>2</sub> test-rig. The high-pressure CO<sub>2</sub> gas from the gascooler discharge (state 1) is the motive fluid to the multiejector. Vapor exiting the AC evaporator (state 8) is drawn as the suction fluid. Ejector lifts CO<sub>2</sub> gas from the AC pressure to receiver pressure (state 4) utilizing a high-pressure stream (state 2). The receiver separates the two vapor-liquid mixture (state 4). The vapor (state 5) is further compressed in the AUX compressor (state 18) and liquid (state 6) is fed to AC (state 7), MT (state 10) and LT (state 12) evaporators after throttling to their corresponding pressures. The vapor at LT evaporator exit (state 13) is compressed separately up to the suction pressure of the MT compressor (state 14). The LT part of the cycle is not connected with the ejector cycles, which means that the compression takes place from the LT evaporator pressure level with no additional boosted pressure lift, unlike the other evaporators. Pure vapor (state 11) from the MT evaporator is then mixed with the discharge high-pressure vapor of the LT compressor (state 14) and the mixed fluid (state 16) is further compressed by the MT compressor up to the gascooler pressure (state 17). During incorporation of the IHX in the system configuration, state 1'-2' represents the expansion of motive fluid in the ejector and state 5'-18' represents the MT compression of the system up to the gas cooler pressure.

### 3.2. Evaporative gascooler

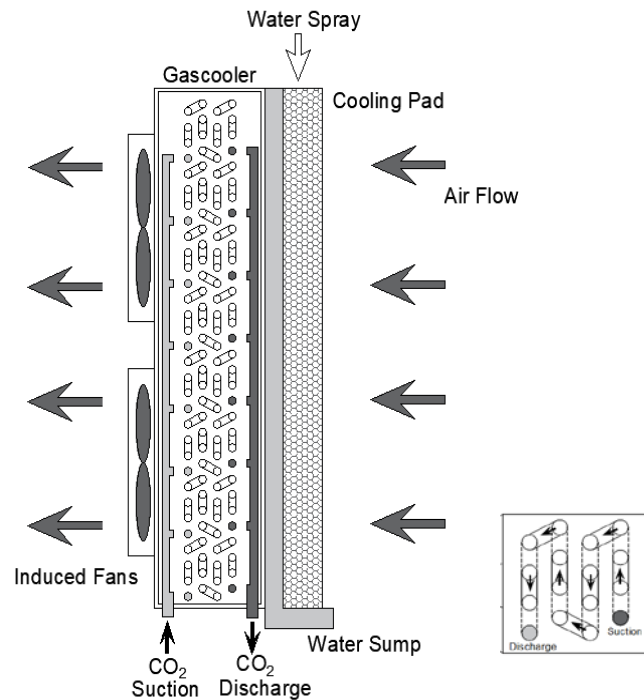


**Figure 6. Evaporative gascooler (side-view).**

Fig. 6 shows the evaporative gascooler (side-view). Gascooler is designed with four parallel stack row arrangements and with eight distribution circuits. Every circuit has sixteen copper material tube passes with common suction and discharge port. Aluminium fins are arranged with equal

spacing to improve the heat transfer between the copper tube and air with an increase in the contact area. Specifications of the CO<sub>2</sub> gascooler are tabulated in Table 3.

**Table 3. Specifications of the CO<sub>2</sub> Gascooler.**

<b>Specifications</b>	<b>Units</b>	<b>Value</b>
<i>Gascooler</i>		
Tube length	<i>m</i>	25.6
Tube material	---	Copper
Fin length	<i>mm</i>	10
Fin material	---	Aluminum
Fin thickness	<i>mm</i>	0.03
Fin spacing	<i>mm</i>	0.03
Distribution circuits	---	8
Coil rows	---	4
Heat exchanger type	---	Fin-tube
Cooling medium	---	Air
Frame height	<i>m</i>	0.81
Frame length	<i>m</i>	1.60
Frame width	<i>m</i>	0.15
<i>Cooling Pad</i>		
Length	<i>m</i>	1.60
Height	<i>m</i>	0.81
Thickness	<i>m</i>	0.15
Material	-	Cellulose
Design/structure	-	Honeycomb
Face area	<i>m</i> <sup>2</sup>	1.157
Evaporative surface area	<i>m</i> <sup>2</sup> <i>m</i> <sup>-3</sup>	370

Two induced type fans are arranged to provide constant airflow through the gascooler coils. Fans are mounted on the solid stainless steel frame of the gascooler. The honeycomb mesh design cooling pad is used in the evaporative cooling arrangement. The water spray is arranged with the support of the distribution plate on the top face of the cooling pad to uniformly distribute water droplets over the pad surface. In principle, the heat transfer properties of air are to be improved by reducing the dry bulb temperature of the air. The cooling pad arrangement is made facing the front panel of the CO<sub>2</sub> gascooler to induce air contact for evaporative cooling. Fig. 7 shows the evaporative cooler with water distribution circuit.

The operation of switching on/off is taken care of by the high pressure (HP) expansion valve opening. The capacity regulation is carried out by on/off switching of the multi-parallel slot ejector



cartages. The six cartages with different loads are designed to operate with an individual solenoid valve to handle different loads. Pressure lifters are also provided in the suction flow entrance to the ejector cartages. The system controllers facilitate both manual and automatic optimization of the gascooler pressure level concerning the gascooler outlet temperature. The facility also has a manual fan controller to vary the air flow rate through the gascooler to adjust the exit refrigerant temperature. An evaporative cooler with provision to insert up to three honeycomb pads of 5 cm each is positioned in front of the gascooler. The same fan is made to draw air through this evaporative cooler. The evaporative cooling system with three pipes one each to a pad with top holes for even water distribution.

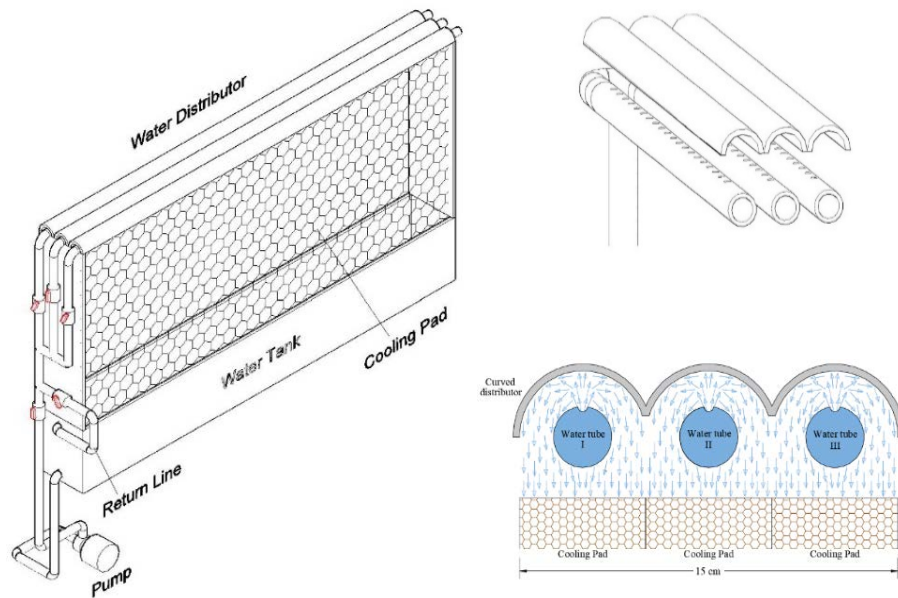


**Figure 7. Evaporative cooler with water distribution circuit.**

#### **4. Experiment procedure**

The CO<sub>2</sub> circuit side parameters such as temperature of evaporators (AC, LT, and MT) receiver pressure (RP), gascooler outlet temperature, etc. are determined in the test-facility service tool. The gascooler pressure is automatically optimized according to the gascooler outlet temperature with the controlling sensor. After directing the system with CO<sub>2</sub> side parameters, the system is turned ON from the main controller (manually). After 15 minutes, loads of the three evaporators are maintained constant by the secondary water/glycol loop. The loads on the evaporators are controlled by the changing mass flow rate of the glycol solution in the secondary loop. The CO<sub>2</sub> system requires approximately two hours to reach a steady state. System performance is evaluated for all steady-state conditions using the hourly data and averaged for a single operational temperature. Properties of CO<sub>2</sub> and glycol solution are obtained from REFPROP software and the CO<sub>2</sub> system operating parameters used for the performance evaluation are tabulated in Table 4.

The Evaporative cooling system introduced in the CO<sub>2</sub> system is tested for the above 40°C system operating temperature. During the procedure, the CO<sub>2</sub> system is set to operate at constant gascooler

outlet temperature by adjusting the gascooler fan speed manually and keeping it constant. After recording the performance of the system for the set operating temperature, the cooling pad thickness is increased to 5, 10, and 15 cm, one by one allowing the gascooler outlet temperature to drop at the fixed gascooler fan speed. The fan speed needs to be reduced manually to achieve the higher gascooler outlet temperature.

**Table 4. CO<sub>2</sub> system operating parameters.**

Operating Parameter	Units	Value/Range
Gascooler temperature	°C	36 to 46
Gascooler pressure	bar	80 to 120
Receiver pressure	bar	45
AC evaporator	°C	+6
LT evaporator	°C	-28
MT evaporator	°C	-6

The performance of the multiejector based CO<sub>2</sub> cooling system for supermarket applications at high ambient temperature is computed using the following equations.

The efficiency of the evaporative cooler ( $\eta_{ec}$ ) is computed by:

$$\eta_{ec} = \frac{T_{inlet,ec} - T_{outlet,ec}}{T_{inlet,ec} - T_{wb}} \quad (1)$$

Coefficient of Performanc (*COP*) of the CO<sub>2</sub> cooling system is computed by,

$$COP = \frac{Q_{AC} + Q_{LT} + Q_{MT}}{P_{AUX} + P_{LT} + P_{MT}} \quad (2)$$

Where, load on the three evaporators AC, LT and MT of the system is computed from the glycol side by:

$$\dot{Q}_{AC} = \dot{m}_{AC} \times c_p \times (T_{AC,outlet} - T_{AC,inlet}) \quad (3)$$

$$\dot{Q}_{LT} = \dot{m}_{LT} \times c_p \times (T_{LT,outlet} - T_{LT,inlet}) \quad (4)$$

$$\dot{Q}_{MT} = \dot{m}_{MT} \times c_p \times (T_{MT,outlet} - T_{MT,inlet}) \quad (5)$$

Power Input Ratio (*PIR*) of the CO<sub>2</sub> cooling system is computed by [42],

$$PIR = \frac{P_{AUX} + P_{LT} + P_{MT}}{P_{AUX,Carnot} + P_{LT,Carnot} + P_{MT,Carnot}} \quad (6)$$

where Carnot power consumption of the three compressors AUX, LT and MT is computed by,

$$P_{AUX,Carnot} = \frac{\dot{Q}_{AC}}{T_{UT,AC}} \times (T_{amb} - T_{UT,AC}) \quad (7)$$

$$P_{LT,Carnot} = \frac{\dot{Q}_{LT}}{T_{UT,LT}} \times (T_{amb} - T_{UT,LT}) \quad (8)$$

$$P_{MT,Carnot} = \frac{\dot{Q}_{MT}}{T_{UT,MT}} \times (T_{amb} - T_{UT,MT}) \quad (9)$$

The utility temperatures ( $T_{UT}$ ) or product temperature assumed for the three evaporators AC, MT and LT are 22°C, 4°C, and -18°C, respectively.

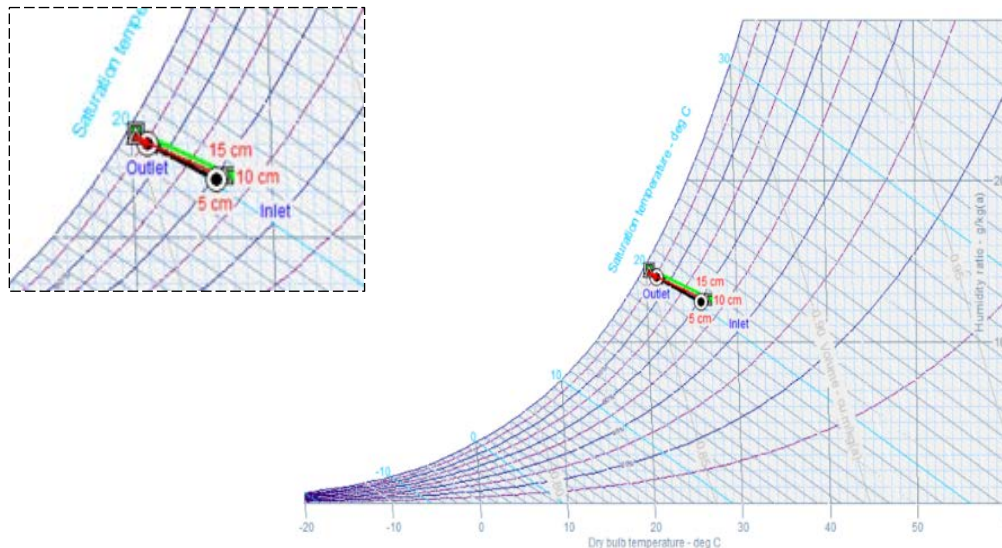
#### 4.1. Uncertainty analysis

In the present experimental study, Type B evaluation of the standard uncertainty is adopted as suggested [43], which is based on the scientific judgment from the information available during measurements of the various parameters. Therefore, the higher and lower limits of the measured quantity from the sensors and uncertainty in the direct measurement is computed using Eq. (10). The combined standard uncertainty of the measured value is estimated using the estimated standard derivation of the results and the uncertainty of the measured quantity and computed using Eq. (11). Uncertainty indirect measurements by the temperature sensor, pressure sensor, and energy meter are 0.69%, 0.119%, and 0.093% respectively.

$$x_i = \frac{\text{Accuracy of the measured value}}{\sqrt{3}} \quad (10)$$

$$u_c^2(y) = \sum_{i=1}^N \left( \frac{\partial f}{\partial x_i} \right)^2 u^2(x_i) \quad (11)$$

### 5. Results and discussion



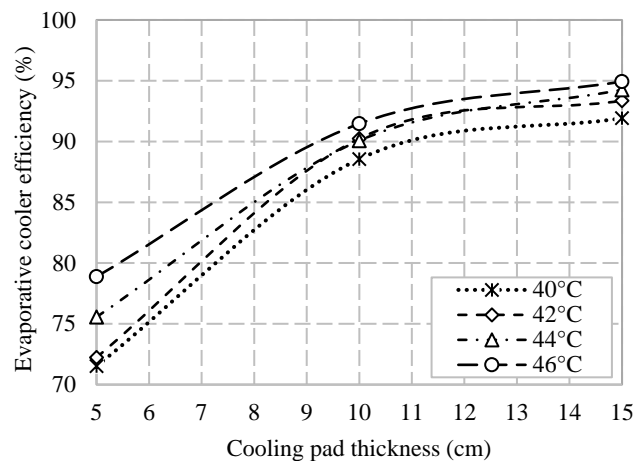
**Figure 8. Condition of air at the inlet and outlet of the evaporative cooler on the psychrometric chart for 5, 10, and 15 cm thick cooling pad.**

Fig. 8 shows the condition of air at the inlet and outlet of the evaporative cooler on the psychrometric chart for 5, 10, and 15 cm thick cooling pad. It is projected that the condition of the air at the inlet is more or less the same for the all three cooling pad thicknesses, as required to compare the overall performance. Moreover, it is observed that as the cooling pad thickness increases, relative humidity (RH) increases and dry bulb temperature (DBT) of the air decreases



at the outlet of the cooling pad, due to an increase in the contact surface area between water and the pad.

Fig. 9 shows the evaporative cooler efficiency with different cooling pad thickness at the various system operating temperatures. The evaporative cooling pad is imposed to evaluate the CO<sub>2</sub> cooling system configuration above 40°C ambient temperature. It is observed that the efficiency of the evaporative cooler increases with pad thickness for the respective gascooler exit temperature. This is ascribed to the fact of increasing contact surface area between water and air in the cooling pad. However, the enhancement in the evaporative cooler efficiency is quite small beyond 10 cm cooling pad thickness. However, the law of diminishing returns applies here and therefore, the benefit approaches zero when the thickness of the cooling pad increases beyond 10 cm. As per the design, the induced fan speed needs to be fixed at a lower value to achieve the higher gascooler outlet temperature. Hence, the resulting low air velocity increases the residence time, thereby the efficiency increase as the gascooler exit temperature is set to higher temperatures. Moreover, the pad thickness of 10 cm is observed to be optimum yielding maximum cooling capacity. The pad thickness has two opposing influences; to decrease the face velocity of air due to an increase in pressure drop and thereby increase the cooling efficiency. Hence the same optimum thickness is obtained, irrespective of the gascooler exit temperature. Therefore, the maximum evaporative cooler efficiency observed as 95%.



**Figure 9. Evaporative cooler efficiency with different cooling pad thickness at the various system operating temperatures.**

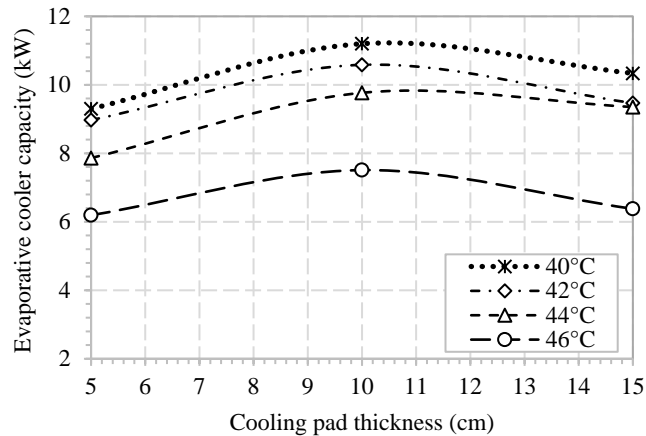


**Figure 10. Evaporative cooler capacity with different cooling pad thickness at the various system operating temperatures.**

Fig. 10 shows the evaporative cooler capacity with different cooling pad thickness at the various system operating temperatures. Within the range of experimental evaluation of the system, the velocity of air is the dominant factor governing the cooler capacity of the evaporator. Therefore, as the figure projects, cooler capacity decreases with an increase in the gascooler outlet temperature. However, further drop in the evaporator cooler capacity is ascribed to the fact of reducing air velocity by increasing the cooling pad thickness (beyond 10cm). This effect is eventually reducing the cooler efficiency. Furthermore, as the system operating temperature increases, the evaporator cooler capacity observed decreasing. Hence, the maximum capacity observed at 10cm cooling pad thickness is ~13 kW.

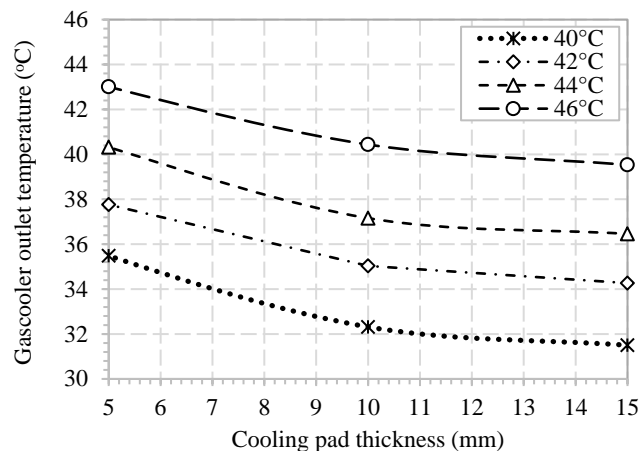


**Figure 11. Gascooler outlet temperature with cooling pad thickness at the various system operating temperatures.**

Fig. 11 shows the gascooler outlet temperature with cooling pad thickness at the various system operating temperatures. It is observed that as the cooling pad thickness increases, the temperature drop in the gascooler increases, ascribed to the reduced DBT of air at the inlet of the gascooler due

to the cooler pad. As the cooling pad thickness increases, the contact surface area between water and air also increases. Therefore, a progressive reduction in temperature is observed for increasing cooling pad thickness. However, the gascooler temperature drop at the outlet is marginal beyond 10cm cooling pad thickness. The maximum drop in temperature at the gascooler outlet is  $\sim 7\text{K}$ .

Fig. 12 shows the gascooler capacity with cooling pad thickness at the various system operating temperatures. As the gascooler outlet temperature decrease, the gascooler capacity also decreases. Hence, a reduction in cooler capacity is observed as the cooling pad thickness increase. Furthermore, as the system operating temperature increases, the gascooler capacity also increases. Therefore, the maximum gascooler capacity observed is 34 kW with a 5cm cooling pad thickness at  $46^\circ\text{C}$  system operating temperature.

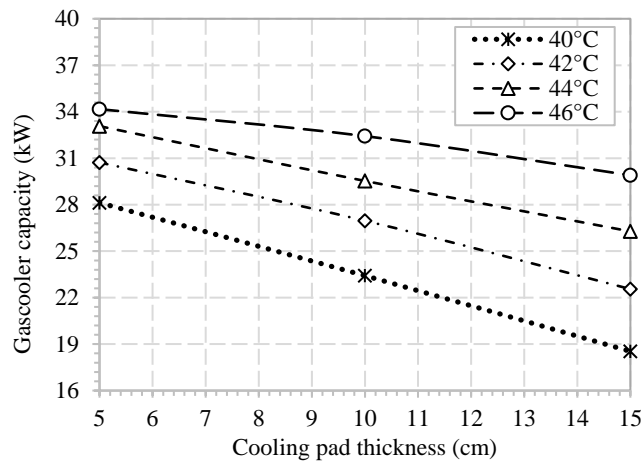


**Figure 12. Gascooler capacity with cooling pad thickness at the various system operating temperatures.**

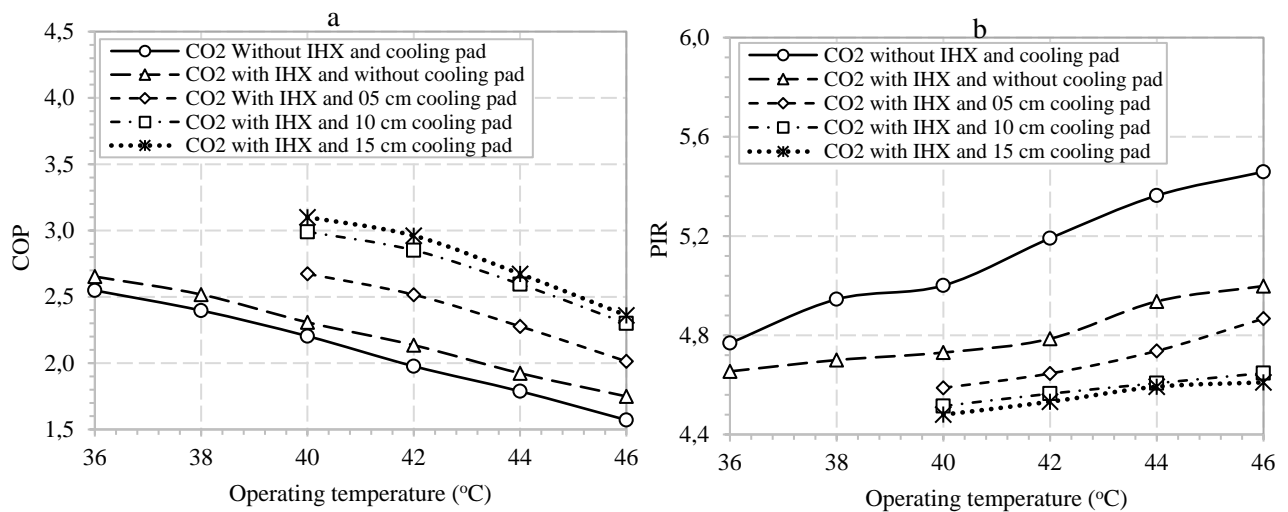


**Figure 13 (a). COP with operating temperatures for the CO<sub>2</sub> cooling system with/without IHX, Figure 13 (b). PIR with operating temperatures for the CO<sub>2</sub> cooling system with/without IHX.**

Fig. 13 shows the COP with the operating temperatures for the CO<sub>2</sub> cooling system with/without IHX and Fig. 13 (b) shows the PIR with the operating temperatures for the CO<sub>2</sub> cooling system with/without IHX. It is observed that as the system operating temperature increases, the COP of the system decreases and PIR of the system increases. This is due to the fact of increasing system operating gascooler temperature and pressure at higher operating temperatures, which requires more work input to the system. Moreover, it is observed that, with the use of IHX in the CO<sub>2</sub> system configuration, COP of the CO<sub>2</sub> cooling system improves and PIR reduces. Moreover, with the use of an evaporative cooling pad in the system above 40°C, further improvement in the overall performance of the CO<sub>2</sub> cooling system is observed due to a reduction in DBT of the air at the gascooler inlet after crossing the evaporative cooler. From the experimental results, it is evident that with the increasing cooling pad thickness, the system performance improves further, however, a small improvement in the overall system performance with the cooling pad thickness is observed beyond 10cm.

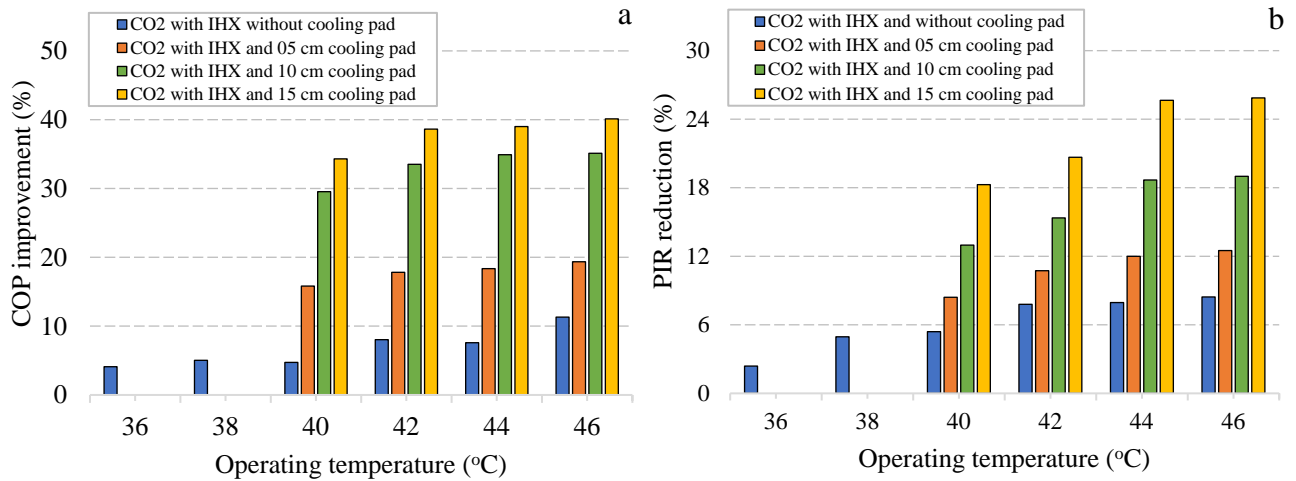


**Figure 14 (a). Improvement in COP with system operating temperatures, Figure 14 (b). Reduction in PIR with system operating temperatures.**

Fig. 14 (a) shows the improvement in COP with system operating temperatures and Fig. 14 (b) shows the reduction in PIR with system operating temperatures. From the experimental results, it is evident that a noteworthy improvement in the overall performance of the CO<sub>2</sub> cooling system is observed with IHX and evaporative cooling in the system configuration. It is observed that, with the support of IHX, maximum COP improvement and PIR reduction are 11% and 8.5% respectively. Moreover, high improvement is observed with the evaporative cooling in CO<sub>2</sub>

gascooler with varying cooling pad thickness. A noteworthy 40% improvement in COP and 26% reduction in system PIR is observed with 15cm cooling pad thickness. However, a marginal increment in COP and reduction in PIR are 4% and 6% are observed above 10cm cooling pad thickness.

## 6. Comparitive analysis

Fig. 15 shows the comparison between the system COP reported and present experimental study. To compare the maximum COP of the CO<sub>2</sub> system, two reported literature are used with the present experimental results.

Firstly, an experimental study was carried out and reported for a CO<sub>2</sub> booster configuration with a high pressure expansion valve in the system configuration [33]. The maximum COP reported for the system was 2.72 at 19°C ambient temperature which is quite low as compared to the present experimental study i.e. 3.1 at 40°C ambient temperature condition. Therefore, ejector technology with the compatibility of the evaporative condenser is proven to be the potential solution at high ambient temperature conditions for a supermarket application. Secondly, a simulation study was carried out using four different ejector based CO<sub>2</sub> system configurations [44]. Among four configurations, an ejector based CO<sub>2</sub> cooling system with three evaporators and two stage compression system (similar to the present experimental study) was reported as outperforming the other three at high ambient temperature conditions upto 40°C. As reported in the literature, at 40°C ambient temperature conditions, the maximum COP of the optimum system observed was 2.8. Whereas for the similar configuration used in the present experimental study with the additional support of evaporative condenser at same ambient temperature/gas cooler outlet temperature is 3.1. Therefore, this offers and projects the evaporative cooler as an add-on solution to the ejector based CO<sub>2</sub> system at high ambient temperature conditions for the supermarket application.

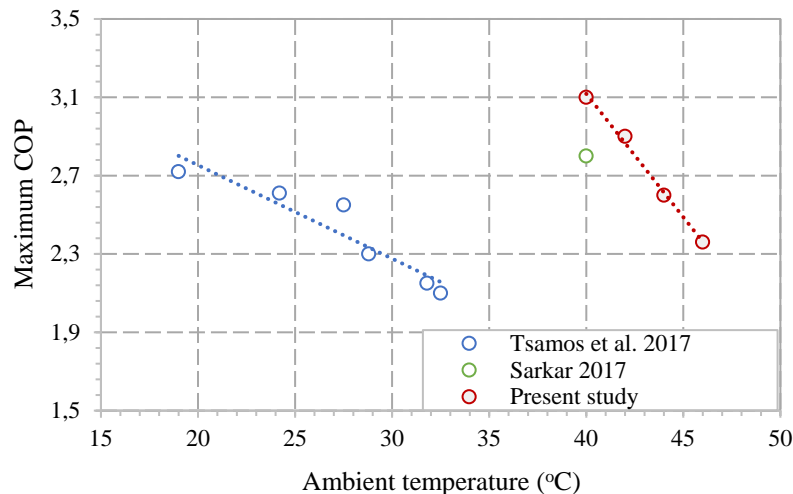


**Figure 15. Comparison between the system COP reported and present experimental study.**

## 7. Conclusions and future scope

In the present experimental study, performance evaluation of a multiejector based CO<sub>2</sub> cooling system with/without IHX and evaporative cooling arrangement are carried out at high ambient temperature conditions up to 46°C for a supermarket application with different cooling pad thickness. The evaporative cooler is designed, fabricated and tested in the CO<sub>2</sub> cooling system for supermarket application above 40°C with the influence of cooling pad thickness 5, 10 and 15cm to reduce the gascooler working pressure to improve the overall performance.

The evaluation is projected in terms of evaporative cooler efficiency, COP and PIR. The evaporative cooler efficiency and COP of the system is associated to define an optimum solution in the present experimental arrangement. It is projected that, after a certain range of thickness of the cooling pad there is a minor enhancement in the evaporative cooler efficiency and the system COP and with respect to which the PIR reduces proportionally. Therefore, in order to obtain the maximum efficiency point of the system, both performance parameters needs to be optimized simultaneously.

The following conclusions are drawn:

- Evaporative cooling in the CO<sub>2</sub> system configuration appeared as an efficient method to improve the overall performance of the system at high ambient temperature conditions.
- The experimental results project the maximum evaporative cooler capacity at 10cm pad thickness. However, a minor improvement is observed in terms of COP and PIR beyond 10cm pad thickness.
- The maximum improvement in COP with the support of IHX and evaporative cooler is 11% and 40% respectively.
- The maximum reduction in the system PIR with the support of IHX and evaporative cooler is 8.5% and 26% respectively.
- Minor enhancement in COP and PIR observed are 4% and 6% respectively above 10cm cooling pad thickness.

From the present experimental study, it is therefore concluded that in future the implementation of evaporative cooling in the multiejector based CO<sub>2</sub> system configuration is a suitable and prominent option for a supermarket application a tropical region at high ambient temperature conditions. Moreover, it would be more interesting and efficient to adopt the present arrangement with the existing R744 systems employed in the various sectors.

## Acknowledgments

The research work presented is part of an Indo-Norwegian project “INDEE” funded by the Ministry of Foreign Affairs, Government of Norway, coordinated by SINTEF, Norway. The authors also like to acknowledge the additional support received from the Department of Science and Technology (DST) under the project: PDF/2017/000083.

## NOMENCLATURE

$c_p$	Specific heat	(kJ/kg K)
$DBT$	Dry bulb temperature	(°C)
$m$	Mass flow	(kg)
$Q$	Evaporator load	(kW)
$RH$	Relative humidity	(%)
$T$	Temperature	(°C)
$UT$	Utility temperature	(°C)

### Abbreviations

$AC$	Air conditioning
$AUX$	Auxiliary
$CO_2$	Carbon dioxide
$COP$	Coefficient of Performance
$HERE$	High ejection ratio ejector
$HP$	High pressure
$IHX$	Internal heat exchanger
$IC$	Intercooler
$LE$	Liquid ejector
$LERE$	Low ejection ratio ejector
$LT$	Low temperature
$MT$	Medium temperature
$PIR$	Power Input Ratio
$RP$	Receiver pressure

### Subscripts

$amb$	ambient
$ec$	evaporative cooler
$wb$	wet-bulb

## REFERENCES

- [1] M. H. Kim, J. Pettersen, and C. W. Bullard, "Fundamental process and system design issues in CO<sub>2</sub> vapor compression systems," *Prog. Energy Combust. Sci.*, vol. 30, no. 2, pp. 119–174, 2004, doi: 10.1016/j.pecs.2003.09.002.
- [2] A. Pearson, "Carbon dioxide - New uses for an old refrigerant," *Int. J. Refrig.*, vol. 28, no. 8, pp. 1140–1148, 2005, doi: 10.1016/j.ijrefrig.2005.09.005.
- [3] E. A. Groll and J. Kim, "Review Article : Review of Recent Advances toward Transcritical CO<sub>2</sub> Cycle Technology," *HVAC&R Res.*, vol. 13, no. 3, pp. 499–520, 2007.
- [4] G. Lorentzen, "Revival of carbon dioxide as a refrigerant," *H V Eng.*, vol. 66, no. 721, pp. 9–14, 1994.
- [5] S. Singh and M. S. Dasgupta, "CO<sub>2</sub> heat pump for waste heat recovery and utilization in dairy industry with ammonia based refrigeration," *Int. J. Refrig.*, vol. 78, pp. 108–120, 2017, doi: 10.1016/j.ijrefrig.2017.03.009.
- [6] B. M. Fronk and S. Garimella, "Water-coupled carbon dioxide microchannel gas cooler for heat pump water heaters :Part II- Model development and validation," *Int. J. Refrig.*, vol. 34, no. 1, pp. 17–28, 2011, doi: 10.1016/j.ijrefrig.2010.05.012.
- [7] P. Y. Yu, K. H. Lin, W. K. Lin, and C. C. Wang, "Performance of a tube-in-tube CO<sub>2</sub> gas cooler," *Int. J. Refrig.*, vol. 35, no. 7, pp. 2033–2038, 2012, doi: 10.1016/j.ijrefrig.2012.06.010.
- [8] D. K. Gupta and M. S. Dasgupta, "Simulation and performance optimization of finned tube gas cooler for trans-critical CO<sub>2</sub> refrigeration system in Indian context," *Int. J. Refrig.*, vol. 38, pp. 153–167, Feb. 2014, doi: 10.1016/j.ijrefrig.2013.09.041.
- [9] Y. T. Ge, S. A. Tassou, I. D. Santosa, and K. Tsamos, "Design optimisation of CO<sub>2</sub> gas cooler/condenser in a refrigeration system," *Appl. Energy*, vol. 160, pp. 973–981, 2015, doi: 10.1016/j.apenergy.2015.01.123.
- [10] K. M. Tsamos, Y. T. Ge, I. D. M. C. Santosa, and S. A. Tassou, "Experimental investigation of gascooler/condenser designs and effects on a CO<sub>2</sub> booster system," *Appl. Energy*, vol. 186, pp. 470–479, 2017, doi: 10.1016/j.apenergy.2016.03.004.
- [11] P.-Y. Yu, W.-K. Lin, and C.-C. Wang, "Performance evaluation of a tube-in-tube CO<sub>2</sub> gas cooler used in a heat pump water heater," *Exp. Therm. Fluid Sci.*, vol. 54, pp. 304–312, Apr. 2014, doi: 10.1016/j.expthermflusci.2014.01.007.
- [12] Y. Yang, M. Li, K. Wang, and Y. Ma, "Study of multi-twisted-tube gas cooler for CO<sub>2</sub> heat pump water heaters," *Appl. Therm. Eng.*, vol. 102, pp. 204–212, 2016, doi: 10.1016/j.applthermaleng.2016.03.123.
- [13] J. Ball and K. Visser, "Applying Evaporative Condensers to Subcritical CO<sub>2</sub> Condensing and Transcritical CO<sub>2</sub> Gas Cooling," in *Industrial Refrigeration Conference & Exhibition San Diego, California*, 2015, pp. 1–48.
- [14] K. A. Joudi and S. M. Mehdi, "Application of indirect evaporative cooling to variable domestic cooling load," *Energy Convers. Manag.*, vol. 41, pp. 1931–1951, 2000.
- [15] G. P. Maheshwari, F. Al-Ragom, and R. K. Suri, "Energy-saving potential of an indirect evaporative cooler," *Appl. Energy*, vol. 69, no. 1, pp. 69–76, 2001, doi: 10.1016/S0306-2619(00)00066-0.
- [16] J. R. Camargo, C. D. Ebinuma, and J. L. Silveira, "Experimental performance of a direct evaporative cooler operating during summer in a Brazilian city," *Int. J. Refrig.*, vol. 28, no. 7, pp. 1124–1132, 2005, doi: 10.1016/j.ijrefrig.2004.12.011.



- [17] L. Fournaison and J. Guilpart, “Numerical model of sprayed air cooled condenser coupled to refrigerating system,” *Energy Convers. Manag.*, vol. 48, pp. 1943–1951, 2007, doi: 10.1016/j.enconman.2007.01.025.
- [18] G. Heidarinejad, M. Bozorgmehr, S. Delfani, and J. Esmaeelian, “Experimental investigation of two-stage indirect/direct evaporative cooling system in various climatic conditions,” *Build. Environ.*, vol. 44, no. 10, pp. 2073–2079, 2009, doi: 10.1016/j.buildenv.2009.02.017.
- [19] J. M. Wu, X. Huang, and H. Zhang, “Theoretical analysis on heat and mass transfer in a direct evaporative cooler,” *Appl. Therm. Eng.*, vol. 29, no. 5–6, pp. 980–984, 2009, doi: 10.1016/j.applthermaleng.2008.05.016.
- [20] G. Heidarinejad, V. Khalajzadeh, and S. Delfani, “Performance analysis of a ground-assisted direct evaporative cooling air conditioner,” *Build. Environ.*, vol. 45, no. 11, pp. 2421–2429, 2010, doi: 10.1016/j.buildenv.2010.05.009.
- [21] A. Fouda and Z. Melikyan, “A simplified model for analysis of heat and mass transfer in a direct evaporative cooler,” *Appl. Therm. Eng.*, vol. 31, no. 5, pp. 932–936, 2011, doi: 10.1016/j.applthermaleng.2010.11.016.
- [22] V. Khalajzadeh, M. Farmahini-farahani, and G. Heidarinejad, “A novel integrated system of ground heat exchanger and indirect evaporative cooler,” *Energy Build.*, vol. 49, pp. 604–610, 2012, doi: 10.1016/j.enbuild.2012.03.009.
- [23] H. Liu, Q. Zhou, Y. Liu, P. Wang, and D. Wang, “Experimental study on cooling performance of air conditioning system with dual independent evaporative condenser,” *Int. J. Refrig.*, vol. 55, pp. 85–92, 2015, doi: 10.1016/j.ijrefrig.2015.03.012.
- [24] H. Hu, T. Magne, P. Neksa, and A. Hafner, “Performance analysis of an R744 ground source heat pump system with air-cooled and water-cooled gas coolers,” *Int. J. Refrig.*, vol. 63, pp. 72–86, 2016, doi: 10.1016/j.ijrefrig.2015.10.029.
- [25] P. Martínez, J. Ruiz, C. G. Cutillas, P. J. Martínez, A. S. Kaiser, and M. Lucas, “Experimental study on energy performance of a split air-conditioner by using variable thickness evaporative cooling pads coupled to the condenser,” *Appl. Therm. Eng.*, vol. 105, pp. 1041–1050, 2016, doi: 10.1016/j.applthermaleng.2016.01.067.
- [26] A. E. Kabeel and M. Abdelgaied, “Numerical and experimental investigation of a novel configuration of indirect evaporative cooler with internal baffles,” *Energy Convers. Manag.*, vol. 126, pp. 526–536, 2016, doi: 10.1016/j.enconman.2016.08.028.
- [27] N. I. Ibrahim, A. A. Al-Farayedhi, and P. Gandhidasan, “Experimental investigation of a vapor compression system with condenser air pre-cooling by condensate,” *Appl. Therm. Eng.*, vol. 110, pp. 1255–1263, 2017, doi: 10.1016/j.applthermaleng.2016.09.042.
- [28] M. H. Shojaeefard, G. R. Molaeimanesh, A. Yarmohammadi, and S. Changizian, “Multi-objective optimization of an automotive louvered fin-flat tube condenser for enhancing HVAC system cooling performance,” *Appl. Therm. Eng.*, vol. 125, pp. 546–558, 2017, doi: 10.1016/j.applthermaleng.2017.07.055.
- [29] A. E. Kabeel and M. M. Bassuoni, “A simplified experimentally tested theoretical model to reduce water consumption of a direct evaporative cooler for dry climates,” *Int. J. Refrig.*, vol. 82, pp. 487–494, 2017, doi: 10.1016/j.ijrefrig.2017.06.010.
- [30] D. Bishoyi and K. Sudhakar, “Experimental performance of a direct evaporative cooler in composite climate of India,” *Energy Build.*, vol. 153, pp. 190–200, 2017, doi: 10.1016/j.enbuild.2017.08.014.
- [31] J. M. Tran, M. Linnemann, M. Piper, and E. Y. Kenig, “On the coupled condensation-

- evaporation in pillow-plate condensers : Investigation of cooling medium evaporation,” *Appl. Therm. Eng.*, vol. 124, pp. 1471–1480, 2017, doi: 10.1016/j.applthermaleng.2017.06.050.
- [32] A. E. Kabeel, M. M. Bassuoni, and M. Abdelgaied, “Experimental study of a novel integrated system of indirect evaporative cooler with internal baffles and evaporative condenser,” *Energy Convers. Manag.*, vol. 138, pp. 518–525, 2017, doi: 10.1016/j.enconman.2017.02.025.
- [33] K. M. Tsamos, Y. T. Ge, I. D. M. C. Santosa, and S. A. Tassou, “Experimental investigation of gas cooler/condenser designs and effects on a CO<sub>2</sub> booster system,” *Appl. Energy*, vol. 186, pp. 470–479, 2017, doi: 10.1016/j.apenergy.2016.03.004.
- [34] M. Kashif Shahzad, M. Ali, N. Ahmed Sheikh, G. Qadar Chaudhary, M. Shahid Khalil, and T. U. Rashid, “Experimental evaluation of a solid desiccant system integrated with cross flow Maisotsenko cycle evaporative cooler,” *Appl. Therm. Eng.*, vol. 128, pp. 1476–1487, 2018, doi: 10.1016/j.applthermaleng.2017.09.105.
- [35] Y. Chen, H. Yan, and H. Yang, “Comparative study of on-off control and novel high-low control of regenerative indirect evaporative cooler (RIEC),” *Appl. Energy*, vol. 225, no. May, pp. 233–243, 2018, doi: 10.1016/j.apenergy.2018.05.046.
- [36] S. Pan *et al.*, “Design and experimental study of a novel air conditioning system using evaporative condenser at a subway station in Beijing, China,” *Sustain. Cities Soc.*, vol. 43, pp. 550–562, 2018, doi: 10.1016/j.scs.2018.09.013.
- [37] J. Wei, J. Liu, X. Xu, J. Ruan, and G. Li, “Experimental and computational investigation of the thermal performance of a vertical tube evaporative condenser,” *Appl. Therm. Eng.*, vol. 160, no. July, p. 114100, 2019, doi: 10.1016/j.applthermaleng.2019.114100.
- [38] X. Zhu, S. Chen, S. Shen, S. Ni, X. Shi, and Q. Qiu, “Experimental study on the heat and mass transfer characteristics of air-water two-phase flow in an evaporative condenser with a horizontal elliptical tube bundle,” *Appl. Therm. Eng.*, vol. 168, no. December 2019, p. 114825, 2020, doi: 10.1016/j.applthermaleng.2019.114825.
- [39] P. Saji Raveendran and S. Joseph Sekhar, “Experimental studies on the performance improvement of household refrigerator connected to domestic water system with a water-cooled condenser in tropical regions,” *Appl. Therm. Eng.*, vol. 179, p. 115684, 2020, doi: 10.1016/j.applthermaleng.2020.115684.
- [40] H. H. Reichert, R. G. Donni, P. S. Schneider, and I. C. A. Junior, “Data driven assessment of a small scale evaporative condenser based on a combined artificial neural network with design of experiment approach,” *Int. J. Refrig.*, vol. 115, pp. 139–147, 2020, doi: 10.1016/j.ijrefrig.2020.02.018.
- [41] C. Zhan, Z. Duan, X. Zhao, S. Smith, H. Jin, and S. Riffat, “Comparative study of the performance of the M-cycle counter-flow and cross-flow heat exchangers for indirect evaporative cooling-paving the path toward sustainable cooling of buildings,” *Energy*, vol. 36, no. 12, pp. 6790–6805, 2011, doi: 10.1016/j.energy.2011.10.019.
- [42] S. Singh, P. M. Maiya, A. Hafner, K. Banasiak, and P. Neksa, “Energy efficient multiejector CO<sub>2</sub> cooling system for high ambient temperature,” *Therm. Sci. Eng. Prog.*, vol. 19, no. January, p. 100590, 2020, doi: 10.1016/j.tsep.2020.100590.
- [43] B. N. Taylor and C. E. Kuyatt, “Guidelines for Evaluating and Expressing the Uncertainty of NIST Measurement Results,” *Natl. Inst. Stand. Technol. Gaithersburg, MD*, p. D.1.1.2, 2001, [Online]. Available: <http://physics.nist.gov/TN1297>.
- [44] J. Sarkar, “Performance analyses of novel two-phase ejector enhanced multi-evaporator

refrigeration systems,” *Appl. Therm. Eng.*, vol. 110, pp. 1635–1642, 2017, doi:  
10.1016/j.applthermaleng.2016.08.163.